Static and Dynamic Effects of the Magnetoelastic Interaction in Terbium and Dysprosium Metals*

D. T. Vigren and S. H. Liu
Institute for Atomic Research and Department of Physics, Iowa State University, Ames, Iowa 50010
(Received 18 January 1971)

A detailed theoretical study has been made of the magnetoelastic perturbation of the spectra of elementary spin and lattice excitations in Tb and Dy metals. The theory was formulated on the basis of an interaction formed from bilinear products of local spin and strain functions. Previous *ad hoc* models appear in certain limits of the theory, giving a coherence to the theoretical picture of magnetoelastic coupling. It is found that uniform magnetostriction causes a smooth transition from "free-lattice" to "frozen-lattice" perturbation of the magnon spectrum depending on the wave vector of the state. The microwave absorption versus magnetic field applied along the hard planar axis of Tb and Dy is calculated. It is found that free-lattice magnons are primarily responsible for low-frequency absorption in Tb below 140 K, and for both low- and high-frequency absorption in Dy below the Curie temperature of that metal. It is shown that the transition from free- to frozen-lattice behavior of the magnon spectrum is essential to the explanation of existing data on the temperature dependence of absorption-peak positions in Tb. The dynamic interaction between spin and lattice waves is derived and used to calculate the mixed-mode splittings in regions of the Brillouin zone of Tb where phonon and magnon dispersion curves cross. The theory predicts well the splitting which occurs where the acoustical-magnon and phonon branches touch, but fails to account for the splitting between the acoustical-magnon and optical-phonon branches. A different coupling mechanism is proposed which may account for the mixing of these branches.

I. EFFECTS OF UNIFORM STRAIN ON MAGNON SPECTRUM

A. Introduction

In the recent past there has been much theoretical and experimental work done to determine the effect of equilibrium strain on the magnon spectrum of the rare-earth metals. Turov and Shavrov[1] in a pioneering paper proposed that in the presence of spin waves the strain tensor may be taken as that of the ground state. They showed, using the equations-of-motion method, that a sizable magnetoelastic contribution to the uniform-mode spectrum is made in this case. Cooper[2] calculated the effects of magnetic anisotropy and elasticity on the magnon spectrum using a Holstein-Primakoff transformation of the spin Hamiltonian. Under the assumption of a "frozen lattice," he obtains a significant magnetoelastic effect. On the other hand, for a free lattice the energy of a uniform-spin oscillation in the basal plane is insensitive to the magnetoelastic effect.

Much experimental work has been done to check the validity of the frozen-lattice approximation. One method is to measure the temperature dependence of the spin-wave energy gap $E(0)$. Callen and Callen[3] have calculated the temperature dependence of the magnetoelastic constants of the "one-ion" type. Coupling constants of importance in Tb and Dy are of this type, with the exception of $\lambda^{\alpha 1}$, which is small. Since the temperature renormalization of the crystal anisotropy is well known,[2] one can measure the temperature dependence of the uniform-mode frequency, subtract the effects of magnetic anisotropy, and deduce the effect, if any, of the magnetoelastic terms. This was done by Marsh and Sievers,[4] who found that both the free- and frozen-lattice models fit their data well, although the frozen-lattice model fits slightly better.

The application of a large dc magnetic field in the magnetically "hard" planar direction of the crystal has the effect of reducing the spin-wave energy gap at $\vec{q}=0$ to a minimum at an applied field equal in magnitude to the effective field of the planar anisotropy, which tends to align the spins along the "easy" direction. Above this applied field, the uniform-mode frequency increases monotonically. If there is no magnetoelastic coupling, the gap is reduced to zero; whereas, if there is coupling, the minimum in $E(0)$ is considerably greater than zero ($\sim 10K$ for Dy at $80\,\mathrm{K}^2$ and where Boltzmann's constant is unity). Nielson *et al.*,[5] in a neutron-diffraction study, report that the energy gap at $\vec{q}=0$ could not be reduced to zero upon application of a strong field in the hard basal direction of Tb metal. This observation seems to substantiate the "frozen-lattice" assumption.

Other groups, using resonance techniques, have studied this same effect. A variable dc field is applied in the hard planar direction and a fixed-microwave-frequency photon beam is incident

normal to the surface of the metal. As the applied field is increased, the uniform-mode spin wave dips and then increases. Strong coupling of the photons to the spin waves occurs when the frequencies are equal. Microwave energies far below the zero-field spin-wave gap are used so that if $E(0)$ dips to zero, then strong on-resonance absorption of the photons should occur at an applied field near the planar anisotropy field, whereas, if the magnetoelastic coupling is important, one should see only broad off-resonance absorption over a considerable range of the applied field.

Bagguley and Liesegang[6] measured strong absorption of $1.8K$ and $0.45K$ microwaves in Tb and Dy. The absorption is characterized by a sharp increase which might be expected in the case of on-resonance absorption, followed by a long tail spanning many kOe of field. The tail is characteristic of broad off-resonance absorption. Rossol[7] did a very detailed investigation of Dy with $1.8K$ microwaves. Wagner and Stanford[8-10] studied both Tb and Dy using $0.45K$ and $4.5K$ radiation. Very recently, Hart and Stanford[11] made a careful study of Tb using $1.0K$ radiation. The observations of these workers agreed essentially with those of Bagguley and Liesegang. The strong and sudden absorption of $0.45K$ and $1.8K$ photons cannot be understood under the assumption of a frozen lattice. Such a frozen-lattice model directly implies off-resonance absorption at these low-driving frequencies. The profile of such absorption would be very broad and flat with no sudden changes in slope, quite unlike the observed profile.[7] Thus, low-frequency ferromagnetic-resonance (FMR) results seem to argue against the applicability of a frozen lattice. Other microwave experiments[8,10] at higher frequencies ($4.5K$) show a temperature dependence of the resonance field in agreement with the frozen-lattice model. At these higher frequencies, however, on-resonance absorption is possible even if the lattice is frozen, and so the shape of the absorption is not inconsistent with the model in this case.

Thus, one is confronted with experimental observations which appear to be contradictory. Neutron-diffraction results clearly conclude that the lattice is frozen. High-frequency resonance absorption also indicates a frozen lattice, but low-frequency resonance absorption cannot be explained unless the lattice is free. It is unreasonable to believe that a crystal can respond totally to a frequency of 40 GHz ($1.8K$), but not at all to a frequency twice as great.

In a previous paper[12] the spin-wave spectrum was studied, assuming that spins are coupled locally to their strain environments. Thus, no *a priori* assumption was made as to whether the macroscopic strains are free or frozen. The resulting spectrum was shown to vary continuously from free- to frozen-lattice behavior, depending on the wave vector of the magnon.

An elaboration of the results obtained previously is made in Sec. I B. In Sec. I C a detailed calculation of microwave absorption is made. It is shown that the wave-vector dependence of the long-wavelength gap has a profound influence on, and is essential to, the correct interpretation of FMR absorption data. On the basis of the locally coupled magnetoelastic theory, a consistent understanding of all existing long-wavelength magnon data obtained through microwave-absorption or neutron-diffraction techniques is attained.

B. Derivation of Spectrum

We begin with the generalized magnetoelastic spin Hamiltonian,[13] which may be separated into a "one-ion" part H_1 and a "two-ion" part H_2:

$$H_1 = -\sum_f \sum_\Gamma \sum_{jj'} B^\Gamma_{jj'}(f) \sum_i \mathcal{E}^{\Gamma j}_i(f) S^{\Gamma j'}_i(f) ,$$
$$H_2 = -\sum_{f,g} \sum_\Gamma \sum_{jj'} D^\Gamma_{jj'}(f,g) \sum_i \mathcal{E}^{\Gamma j}_i(f,g) S^{\Gamma j'}_i(f,g) . \tag{1}$$

Here f, g are position indices, Γ defines the irreducible representations of the crystal point group, i specifies the basis set of the representation, j and j' are used if more than one basis set carries the representation, $S(f)$ and $S(f,g)$ are the usual one- and two-ion spin functions defined by Callen and Callen,[3] and $B(f)$ and $D(f,g)$ are the one- and two-ion coupling coefficients. The local strains are defined as follows:

$$\mathcal{E}_{xx}(f,g) = (X_f - X_g)(x_f - x_g) , \tag{2}$$

$$\mathcal{E}_{xy}(f,g) = \tfrac{1}{2}[(X_f - X_g)(y_f - y_g) + (Y_f - Y_g)(x_f - x_g)] , \tag{3}$$

and similarly for the other Cartesian components. Here $\vec{R}_f = (X_f, Y_f, Z_f)$ is the position vector of the fth ion in the unstrained crystal; $\vec{r}_f = (x_f, y_f, z_f)$ is the displacement of the fth ion from its unstrained equilibrium position. The z axis of the Cartesian coordinates is taken along the crystal $\hat{c}$ axis, and the x axis is taken along the easy planar direction. The one-ion strains are defined simply by a summation over nearest-neighbor distances δ:

$$\mathcal{E}(f) = \sum_\delta \mathcal{E}(f, f+\delta) . \tag{4}$$

The displacements $\vec{r}_f$ which appear in the local strain functions consist of two parts. One gives rise to magnetostriction produced by the spin order; the other gives rise to normal modes of vibration about the strained equilibrium positions. In this section we treat the effect of the magnetostriction, which shifts the magnon energy spectrum. In a later section we treat the coupling of spin and lattice vibrational modes in the production

of mixed-mode states. In treating the effects of magnetostriction we initially assume that the lattice is infinite, and that the crystal is capable of responding so as to produce macroscopic strains that minimize the elastic energy. Later we refine the theory so as to account for finite crystal dimensions and a limited response time.

For applications to Dy and Tb, three irreducible representations of the hcp point group are important. In Eq. (1) H_1 is applied to γ, ϵ, and $\alpha 2$, and H_2 is applied to $\alpha 1$.[14,15] The sum on g is taken over nearest neighbors only, and the coefficients B^Γ and D^Γ are assumed to be independent of atomic site. In the ferromagnetic phase a uniform strain exists and may be coupled to the local spin functions. For a uniform strain the local strain functions reduce to ordinary strain components and the coefficients B^Γ and D^Γ reduce to the coefficients of Callen and Callen,[3] denoted by $\tilde{B}^\Gamma$ and $\tilde{D}^\Gamma$. Treating the spins as classical quantities and minimizing the total elastic Hamiltonian with respect to the strain components, we obtain an effective spin Hamiltonian. This spin Hamiltonian is then transformed to spin-wave operators by a Holstein-Primakoff transformation. For terms in Eq. (1) of the γ representation, the result of this labor is[12]

$$H^\gamma = \frac{(\tilde{B}^\gamma)^2 NS^2}{4c^\gamma}\left(\sum_{\vec{q}} (S-\tfrac{1}{2})(6a_{\vec{q}}^\dagger a_{\vec{q}} - a_{\vec{q}}^\dagger a_{-\vec{q}}^\dagger - a_{\vec{q}} a_{-\vec{q}}) - 2S(2a_0^\dagger a_0 - a_0^\dagger a_0^\dagger - a_0 a_0)\right), \quad (5)$$

where only the quadratic terms in magnon operators are retained. In an exactly similar manner we obtain for the ϵ and α representations

$$H^\epsilon = -\frac{(\tilde{B}^\epsilon)^2 NS^3}{2c^\epsilon}(2a_0^\dagger a_0 + a_0 a_0 + a_0^\dagger a_0^\dagger),$$
$$H^\alpha = A_q^\alpha a_q^\dagger a_q + \tfrac{1}{2}B_q^\alpha (a_q^\dagger a_q^\dagger + a_q a_q). \quad (6)$$

Here

$$A_q^\alpha = -\sqrt{3}NS^3\left[\frac{\tilde{B}_{12}}{c_{11}}\left(\tilde{B}_{11} - \frac{\tilde{B}_{12}}{2\sqrt{3}}\right) + \frac{\tilde{B}_{22}}{c_{22}}\left(\tilde{B}_{21} - \frac{\tilde{B}_{22}}{2\sqrt{3}}\right)\right] + NS^3\left[\frac{1}{c_{11}}\left(\tilde{B}_{11} - \frac{\tilde{B}_{12}}{2\sqrt{3}}\right)\left(2\tilde{B}_{11} + \frac{\tilde{B}_{21}}{\sqrt{3}}\right) + \frac{1}{c_{22}}\left(\tilde{B}_{21} - \frac{\tilde{B}_{22}}{2\sqrt{3}}\right)(3\tilde{B}_{21} + 2\sqrt{3}\,\tilde{B}_{11})\right]\left(1 - \cos\frac{qc}{2}\right),$$

$$B_q^\alpha = -\sqrt{3}NS^3\left[\frac{\tilde{B}_{12}}{c_{11}}\left(\tilde{B}_{11} - \frac{\tilde{B}_{12}}{2\sqrt{3}}\right) + \frac{\tilde{B}_{22}}{c_{22}}\left(\tilde{B}_{21} - \frac{\tilde{B}_{22}}{2\sqrt{3}}\right)\right],$$

where c is the hcp lattice parameter, and the subscripted c's refer to the elastic constants of the α representation. Here we have assumed $\vec{q} = q\hat{c}$, and will consider only magnon propagation in this direction throughout the remainder of this manuscript. The cosine-dependent term is a direct consequence of the two-ion nature of the $\alpha 1$ representation. It arises from the fully symmetric magnetoelastic term, and so contributes a term in the total Hamiltonian identical in form to the Heisenberg exchange term. We have calculated the numerical value of the term using the data of Rhyne and Legvold,[16] and find that it accounts for less than 10% of the magnitude of $(J_q - J_0)$ deduced from the spin-wave data in the region of small q. Here J_q refers to the Fourier transform of the exchange energy. Insufficient magnetostriction data were available for Dy metal to do a similar analysis, but one would expect a result similar to that of Tb. Thus, it seems safe to neglect the "two-ion" magnetoelastic interaction in the extraction of J_q from the spin-wave spectrum of these metals.

The magnetoelastic terms H^γ, H^ϵ, and H^α are added to the exchange and anisotropy terms derived by Cooper,[2] and the total Hamiltonian is diagonalized. The result for the magnon energy at zero temperature and field is[2]

$$E(\vec{q}) = [(A_{\vec{q}} + B_{\vec{q}} + \Delta_{\vec{q}}^+)(A_{\vec{q}} - B_{\vec{q}} + \Delta_{\vec{q}}^-)]^{1/2}. \quad (7)$$

For $\vec{q}$ in the c direction ($\vec{q} = q\hat{c}$), we have

$$A_q = 2S(J_0 - J_q) - P_2 S - 21P_6^6 S^5,$$
$$B_q = -P_2 S + 15P_6^6 S^5,$$
$$\Delta_q^+ = \frac{c^\gamma(\lambda^\gamma)^2}{2NS} - \frac{\sqrt{3}}{NS}\left[c_{11}\left(\lambda_{11}\lambda_{12} - \frac{(\lambda_{12})^2}{2\sqrt{3}}\right) + c_{22}\left(\lambda_{21}\lambda_{22} - \frac{(\lambda_{22})^2}{2\sqrt{3}}\right)\right] - \frac{c^\epsilon(\lambda^\epsilon)^2}{NS}\,\delta_{q0},$$
$$\Delta_q^- = (1 - \delta_{q0})\,c^\gamma(\lambda^\gamma)^2/NS.$$

The symbols J_q, P_2, P_6^6, $\lambda_{jj'}^\Gamma$ are the Fourier transform of the exchange interaction, the twofold and sixfold anisotropy constants, and the magnetostriction, respectively. A discontinuity in the spin-wave spectrum appears at $q = 0$ due to the terms $\Delta_q^\pm$.

The physical origin of the discontinuity may be understood as follows: When a spin precesses about its equilibrium position, it tends to drag the lattice distortion with it. For a spin wave of infinite wavelength, the lattice distortions of all unit cells must move in phase, so that they add up to a macroscopic strain which follows the precession of the magnetization. Clearly, the strain configuration relative to the magnetization direction is identical at each instant of time to that of the ground-state ferromagnet. That is to say, it costs no magnetoelastic energy to excite the spin system, and the energy gap at zero wave vector is due solely to the magnetic anisotropy produced by the crystal field. This situation corresponds to a free-lattice model for the magnetoelastic coupling. In the event that a spin wave of finite wavelength is excited, the periodic spin component induces only a periodic dis-

tortion at the surface of the crystal.[13] For a wavelength equal to the thickness of the crystal, the penetration of the distortion is complete. For some shorter wavelength, however, the distortion is sufficiently confined to the surface of the crystal so that the bulk strain is induced by the ferromagnetic spin component. This volume strain is essentially the same as that produced by the ground-state magnetization, and is constant in time. The spins now oscillate about this fixed strain axis, creating magnetoelastic free energy and giving rise to a magnetoelastic contribution to the energy gap. This situation corresponds to the frozen-lattice model. Thus, the lattice behavior varies from free to frozen lattice within a very small range of $\vec{q}$, where $\vec{q}$ is the wave vector of the magnons. Under the assumption of an infinitely large specimen, this rapid variation results in a discontinuity in the magnon spectrum from $\vec{q}=0$ to $\vec{q}=0^+$, where $\vec{q}=0^+$ is taken to mean the shortest finite magnon wave vector as determined by the inverse dimensions of the specimen.

The energy of the $q=0$ mode agrees with the free-lattice theory, and that of the $q=0^+$ mode agrees with the frozen-lattice theory. Both come out naturally as consequences of the local spin-lattice interaction. In Table I we give the estimated sizes of the spin-wave gaps for Tb and Dy at zero field. In calculating these values, the data of Fisher and Dever[17] were used for the elastic constants, and the data of DeSavage and Clark[15] and Rhyne and Legvold[16] were used for the magnetostriction constants of Tb. The Dy magnetostriction constants were taken from the data of Clark *et al.*[14] Note that the free-lattice gap is always smaller than the frozen-lattice gap, as expected.

The temperature renormalization of the spin-wave gaps is easily accomplished using the "one-ion" theory of Callen and Callen[3] described above. The magnetoelastic terms are renormalized according to $(\hat{I}_{5/2})^2$, where the function $\hat{I}_{5/2}$ is a reduced hyperbolic Bessel function, whose argument is the inverse Langevin function of the relative magnetization. This renormalization is not quite correct since the $\alpha 1$ representation should be renormalized according to a "two-ion" scheme. However, the $\alpha 1$ representation contributes only a small term to the factor in Eq. (7) containing the large axial anisotropy term $-2P_2S$, so that the result is negligibly affected by this error. The temperature renormalization of the planar anisotropy depends on the origin of this anisotropy. Recent neutron-diffraction work by Nielsen and co-workers[5, 18] showed that virtually all the planar anisotropy of Tb metal arises from hexagonally symmetric second-order magnetostriction. Thus the renormalization should be $\hat{I}_{9/2}\hat{I}_{5/2}$.[2, 3] In Dy metal, however, one might expect that the crystal field is more important in producing the anisotropy, since Dy ions have a higher orbital angular momentum than Tb ions, and hence are capable of stronger interaction with the crystal field. We assume that the planar anisotropy of Dy arises solely from the crystal field interaction, and use the renormalization $\hat{I}_{13/2}$.[3] Then, using an oblate spheroid geometry for the samples, we can generalize Eq. (7) to the case of finite field and temperature[2]:

$$E(q\sim 0)=\{[-2P_2S\hat{I}_{5/2}\sigma^{-1}-6P_6{}^6S^5(\cos 6\theta)\hat{I}_{13/2}\sigma^{-1} + g\mu_B(H+4\pi M-D_xM)\cos(\pi/6-\theta) + \Delta_0^+\hat{I}_{5/2}{}^2\sigma^{-1}][-36P_6{}^6S^5(\cos 6\theta)\hat{I}_{13/2}\sigma^{-1} + g\mu_B H\cos(\pi/6-\theta)+\Delta_0^-\hat{I}_{5/2}{}^2\sigma^{-1}]\}^{1/2}. \quad (8)$$

The equation is written for Dy metal. In the case of Tb we make the replacement $\hat{I}_{13/2}\to\hat{I}_{9/2}\hat{I}_{5/2}$ in Eq. (8) and all related formulas. D_x is a demagnetization factor, $\vec{M}$ is the net magnetization, σ is the relative magnetization, and θ is the angle between $\vec{M}$ and the easy axis in the basal plane. The angle θ is implicitly a function of the applied field, and is given as a solution to the transcendental Eq. (7):

$$\frac{\sin 6\theta}{6\sin(\pi/6-\theta)}=\frac{g\mu_B H}{36P_6{}^6S^5\hat{I}_{13/2}\sigma^{-1}}\ .$$

The H that appears here and in Eq. (8) is the external field. The relevant hyperbolic Bessel functions were evaluated in closed form using the recursion formulas found in the N. B. S. *Table of Functions*. The final expressions used were

$$\hat{I}_{5/2}(z)=1-3\sigma/z\ ,$$

$$\hat{I}_{9/2}(z)=1+\frac{45}{z^2}+\frac{105}{z^4}-(\coth z)\left(\frac{10}{z}+\frac{105}{z^3}\right)\ ,$$

$$\hat{I}_{13/2}(z)=\left(1+\frac{210}{z^2}+\frac{4725}{z^4}+\frac{10395}{z^6}\right) -(\coth z)\left(\frac{21}{z}+\frac{1260}{z^3}+\frac{10395}{z^5}\right).$$

Here $\mathcal{L}(z)=\sigma$, where $\mathcal{L}$ is the Langevin function.

The values of $\sigma(\vec{H}, T)$ were taken from the isothermal magnetization curves of Behrendt and Legvold[19] for Dy, and of Hegland *et al.*[20] for Tb. These curves were plotted against the internal field, so care was taken to convert to the external field, using the demagnetizing factors of an oblate spheroid.

The spin-wave gaps are plotted against the ex-

TABLE I. Energy gaps for Tb at $T=0$ K and Dy at $T=78$ K.

	$E(0)$	$E(0^+)$
Tb	14.0K	19.4K
Dy	6.8K	10.2K

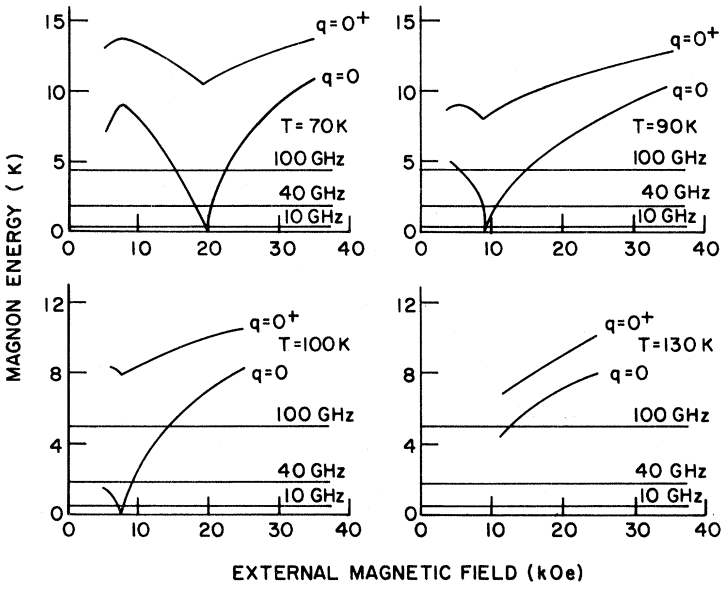

FIG. 1. Magnon energy vs external magnetic field for Dy metal.

ternal field in Figs. 1 and 2 for Dy and Tb, respectively. The curves are drawn for fields above the domain-alignment field only. A strong dip in the free-lattice mode $E(0)$ occurs when the external field approaches the effective planar anisotropy field. This effective field arises from magnetoelastic and crystal field anisotropy in the basal plane, and is represented by the applied-field-independent terms in the second factor under the radical sign in Eq. (8). As the temperature increases, this effective field decreases until it falls below the domain-alignment field of the sample. This occurs at 110 K for Dy, and at 140 K for Tb. The frozen-lattice mode $E(0^+)$ is rather flat over most of the field sweep in the low-temperature ferromagnetic regimes of these metals. Also, this mode lies far above the applied microwave energies, which are indicated by horizontal lines in the figures, with the exception of a sharp drop near the domain-alignment field in Tb. Thus, at low temperatures one expects frozen-lattice excitations to cause a broad off-resonance absorption spanning most of the field range with no sharp increase at the effective planar anisotropy field. On the other hand, one expects strong on-resonance coupling of the free-lattice modes to the microwaves near the planar anisotropy field. Rossol[7] observes strong absorption of 37-GHz radiation at 78, 86, and 91 K

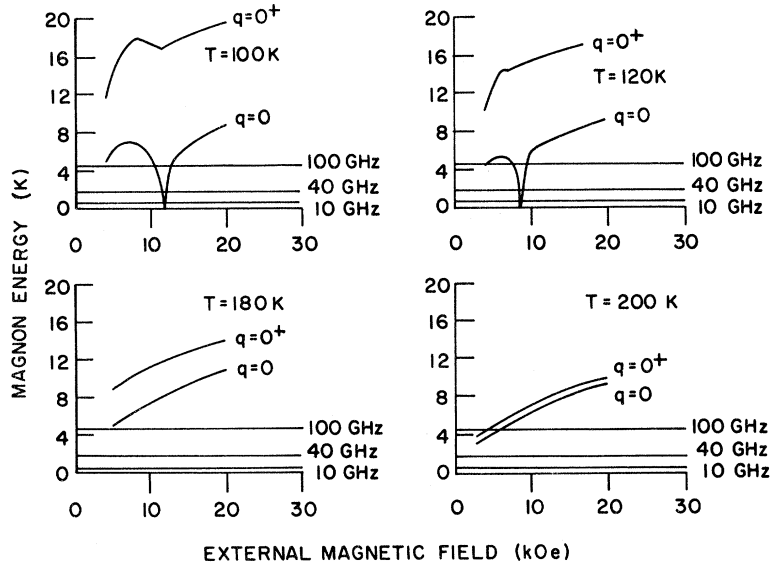

FIG. 2. Magnon energy vs external magnetic field for Tb metal.

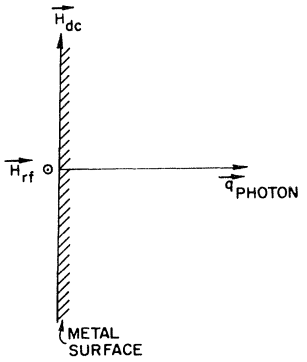

FIG. 3. Geometry of a typical FMR experiment. The crystal is cut so that the basal plane lies parallel to the metal surface.

near the planar anisotropy field in Dy metal. In a recent microwave study at 24 GHz, Hart and Stanford[11] observe sharp absorption peaks near the planar anisotropy field between 70 and 140 K in Tb metal. These experiments suggest strongly that the free-lattice magnons are responsible for low-frequency ferromagnetic resonance absorption. In Sec. IC, a detailed calculation of microwave absorption is made for Dy and Tb, and the relative importance of the free- and frozen-lattice magnons to this process at various frequencies, temperatures, and applied fields is determined.

C. Interpretation of Experiments

In analyzing the data of neutron diffraction and ferromagnetic resonance, it is important to see which way the lattice behaves in the presence of the magnetic disturbance created by the neutron or photon probes. An important consideration is over what macroscopic distance the uniform magnetostriction, which minimizes the instantaneous elastic energy, can be realized by the crystal. Since strain is a differential quantity, the deformation at any interior point $\vec{r}$ depends on the deformation of the surface atoms and its distance from the surface. Such information is carried from the surface with a velocity of 10^6 cm/sec in Tb (the speed of sound). Microwave and neutron-diffraction experiments typically excite magnons of frequency 10^{10} cps, so that only atoms within a distance of 10^{+4} Å of the surface can receive this information and can distort in accordance with the equilibrium strains. Thus, if the probe which creates the spin disturbance penetrates deeply into the crystal, as in the case of neutron diffraction, the bulk of the lattice cannot respond and remains frozen. Thus, one excites frozen-lattice magnons in a neutron-diffraction experiment. In ferromagnetic resonance on metals, however, the photons can only penetrate the surface a distance d, called the radiation skin depth. In Tb and Dy this is about 10^4 Å for 10-GHz radiation, so that macroscopic strains are easily formed in the region where the microwaves couple to the spin system, making free-lattice behavior possible.

In this section we calculate in detail the microwave absorption expected in resonance experiments in which a large dc magnetic field is applied along the hard axis in the basal plane of a hcp metal. Typically, these are the above-mentioned experiments of Bagguley, Rossol, Wagner, and Hart.

The experimental configuration is as shown in Fig. 3. The crystal is cut so that the $\hat{c}$ direction is perpendicular to the metal surface. The photon beam is incident along this direction. The radiation is linearly polarized in the plane of the metal surface, and the amplitude of the wave is damped out in a skin depth d. A dc magnetic field is applied along the hard-crystal direction in the basal plane, in a direction perpendicular to the polarization of the photon beam (which is taken to be in the $\hat{x}$ direction for this calculation). The spin system is assumed to be aligned fully along the applied field in the ground state.

Let $W_{\beta\beta'}$ = probability/time of transition from state β to β', where β and β' are states of the spin system. Then

$$W_{\beta\beta'} = (2\pi/\hbar)\,|\langle\beta'|V|\beta\rangle|^2\delta(E_\beta - E_{\beta'} + \hbar\omega)\ ,$$

as is given by Fermi's Golden Rule for the absorption of quantum $\hbar\omega$ from a time-dependent electromagnetic perturbation field. We calculate $W_{\beta\beta'}$ for the photon-magnon interaction in an optical pumping experiment. The microwave magnetic field intensity inside the metal is

$$\vec{H} = (H_0 e^{-z(1+i)/d} e^{i\omega t} + \text{c.c.})\,\hat{x}\ ,$$

and the perturbation potential is

$$\begin{aligned} V(t) &= -\textstyle\sum_f \vec{\mu}_f \cdot \vec{H}(\vec{R}_f, t) \\ &= -\textstyle\sum_f (\mu_{fx} H_0 e^{-z_f(1+i)/d} e^{i\omega t} + \text{c.c.})\ . \end{aligned}$$

Here $\vec{\mu}_f$ is the magnetic moment on the fth site. We assume that other processes are more favorable to magnon decay than the photon-magnon interaction, so we only consider absorption processes. Therefore we omit the complex conjugate term and obtain

$$V = -\textstyle\sum_f (\mu_{fx} H_0 e^{-z_f(1+i)/d})\ .$$

Now we have

$$S_{fx} = -(\mu_{fx}/g\mu_B) = \tfrac{1}{2}(S_f^+ + S_f^-) = (\tfrac{1}{2}S)^{1/2}(a_f + a_f^\dagger)\ .$$

Here g is gyromagnetic ratio, μ_B is Bohr magneton, and a_f is a boson spin-annihilation operator on the fth site. Substitution of spin-deviation operators for μ_{fx} yields

$$V = (\tfrac{1}{2}S)^{1/2} g\mu_B H_0 \textstyle\sum_f e^{-z_f(1+i)/d}(a_f + a_f^\dagger)\ .$$

Now Fourier transform the boson operators:

$$V = H_0 \sum_f \sum_{\vec{q}} e^{-Z_f(1+i)/d}(a_{\vec{q}} e^{-i\vec{q}\cdot\vec{R}_f} + a_{\vec{q}}^\dagger e^{i\vec{q}\cdot\vec{R}_f})(S/2N)^{1/2} g\mu_B .$$

Summing first over the X_f and Y_f components of $\vec{R}_f$, then over q_x and q_y, we obtain

$$V = \left(\frac{SN}{2}\right)^{1/2} g\mu_B H_0 \sum_{Z_f} \sum_q e^{-Z_f(1+i)/d} \times (a_q e^{-iqZ_f} + a_q^\dagger e^{iqZ_f}) \frac{1}{N_z} .$$

Here N_z is the number of unit cells in the z direction and $N = N_x N_y N_z$. The suppressed notation $q_z \equiv q$ and $a_q \equiv a_{0,0,q}$ is also used.

Now the damping distance $d \ll L_z$, the thickness of the crystal. So one may take the upper limit of the sum on Z_f as ∞ with negligible error, and convert the sum to an integral:

$$\sum_{Z_f} \to \int_0^\infty \frac{dz}{c} ,$$

c being the hcp lattice parameter. Then using $N_z c = L_z$, we can write

$$V = iH_0\left(\frac{SN}{2}\right)^{1/2} \frac{g\mu_B}{L_z} \times \sum_q \left[\frac{a_q}{(q + 1/d - i/d)} + \frac{a_q^\dagger}{(1/d - q - i/d)}\right] . \quad (9)$$

Now we make a Bogoliubov transformation from the boson operators a_q to the magnon operators α_q:

$$a_q = u_q \alpha_q - v_q \alpha_{-q}^\dagger . \quad (10)$$

Here u_q and v_q are c numbers and satisfy

$$u_q^* = u_{-q} = u_q, \qquad v_q^* = v_{-q} = v_q .$$

Substitution of Eq. (10) into the commutation relation $[a_q, a_q^\dagger] = 1$, and requirement that α_q satisfy the boson commutation rules, gives the relation

$$u_q u_q^* - v_q v_q^* = 1 . \quad (11)$$

The requirement that the Hamiltonian of Eq. (7) be diagonal in α_q,

$$H_m = \sum_q E(q)\, \alpha_q^\dagger \alpha_q ,$$

with

$$E(q) = [(A_q)^2 - (B_q)^2]^{1/2} ,$$

gives further relations among the c numbers:

$$u_q u_q^* + v_q v_q^* = A_q/E(q) , \qquad 2u_q v_q = B_q/E(q) . \quad (12)$$

Then, under the transformation of Eq. (10), Eq. (9) becomes

$$V = iH_0\left(\frac{SN}{2}\right)^{1/2} \frac{g\mu_B}{L_z} \sum_q \left[(u_q^* - v_{-q})\left(-q + \frac{1}{d} - \frac{i}{d}\right)^{-1} \alpha_q^\dagger + (u_q - v_{-q}^*)\left(q + \frac{1}{d} - \frac{i}{d}\right)^{-1} \alpha_q\right] .$$

Using Eqs. (11) and (12), the square of the matrix element for the absorption of one photon and the creation of one magnon of wave number q is

$$|\langle n_q + 1|\, V\, |n_q\rangle|^2 = |H_0|^2 \frac{SN}{2} \frac{g^2\mu_B^2}{L_z^2} \times \frac{(n_q + 1)}{[(1/d - q)^2 + 1/d^2](A_q + B_q)} .$$

Here $n_q = (e^{\beta E(q)} - 1)^{-1}$, and $E(q) = (E_{\beta'} - E_\beta)$ is the magnon energy with wave vector q. We assume that $n_q \approx kT/E(q) \gg 1$ in all regions of temperature and wave vector of interest. Then the transition probability $W_\omega(q)$ is given by

$$W_\omega(q) = \frac{NS\pi}{\hbar} \frac{g^2\mu_B^2}{L_z^2} |H_0|^2 \frac{kT}{A_q + B_q} \frac{\delta(\hbar\omega - E(q))}{(1/d - q)^2 + 1/d^2} . \quad (13)$$

Neutron-diffraction studies show that the magnon spectrum is broadened somewhat at $q = 0$, so we will assume a Lorentzian broadening of the energy at fixed wave vector. To account for this in Eq. (13) we make the replacement

$$\delta(\hbar\omega - E(q)) \to \frac{\gamma_m/\pi}{[\hbar\omega - E(q)]^2 + \frac{1}{4}\gamma_m^2} .$$

Here γ_m is the width of the magnon spectrum. Since $\vec{H}$ is parallel to the metal surface, it is continuous across it. Thus H_0 is the amplitude of the incident radiation, and $|H_0|^2$ is related to the element of area under the intensity distribution of the photons in the following way:

$$\vec{S}_{av} = I(\omega)\, d\omega = (c_0/8\pi)\, \mathrm{Re}(\vec{E} \times \vec{B}^*) = (c_0/8\pi)|H_0|^2 .$$

Here $\vec{S}_{av}$ is the time-averaged Poynting vector at the metal surface and c_0 is the speed of light. Thus we have

$$|H_0|^2 = (8\pi/c_0) I(\omega)\, d\omega .$$

Now assume a Lorentzian shape for the photon spectrum:

$$I(\omega) = (\gamma_{ph}/\pi)[(\omega - \bar{\omega}_{rf})^2 + \tfrac{1}{4}\gamma_{ph}^2]^{-1} .$$

Here γ_{ph} is the width of the spectrum and $\bar{\omega}_{rf}$ is the center frequency of the incident radiation. Making the above replacements and substitutions in Eq. (13) and integrating over all photon frequencies we obtain

$$W(q) = \frac{NS\pi g^2\mu_B^2}{\hbar^2 L_z^2 c_0} \frac{kT}{A_q + B_q} \left[\left(\frac{1}{d} - q\right)^2 + \frac{1}{d^2}\right]^{-1} \frac{\gamma_{ph} + \gamma_m}{\pi} \times \left[\left(\bar{\omega}_{rf} - \frac{E(q)}{\hbar}\right)^2 + \frac{(\gamma_{ph} + \gamma_m)^2}{4}\right]^{-1} .$$

The photon beam is usually generated in a klystron tube and has a narrow linewidth. So we assume

$\gamma_m \gg \gamma_{ph}$. Then the transition rate from a state with n_q magnons to (n_q+1) magnons becomes

$$W(q) = \frac{N_0 kT}{L_z(A_q+B_q)}\left[\frac{\gamma_m^2}{4}+\left(\bar{\omega}_{rf}-\frac{E(q)}{\hbar}\right)^2\right]^{-1} \times\left[\frac{1}{d^2}+\left(\frac{1}{d}-q\right)^2\right]^{-1}.$$

Here

$$N_0 = 8NSg^2\mu_B^2\pi\gamma_m/c_0 L_z\hbar^2$$

and is independent of L_z by virtue of N in the numerator.

The transition rate to the $q=0$ state is then

$$W(0) = \frac{N_0 kTd^2}{(A_0+B_0)L_z}\left[\frac{\gamma_m^2}{4}+\left(\bar{\omega}_{rf}-\frac{E(0)}{\hbar}\right)^2\right]^{-1}. \quad (14)$$

The total transition rate to the states $q\neq 0$ is given by

$$W_T = \frac{L_z}{2\pi}\int_{0^+}^{\pi/c} dq\, W(q) = \frac{N_0 kT}{2\pi} I_d, \quad (15)$$

where

$$I_d = \int_{0^+}^{\pi/c}\frac{dq}{A_q+B_q}\left[\frac{\gamma_m^2}{4}+\left(\bar{\omega}_{rf}-\frac{E(q)}{\hbar}\right)^2\right]^{-1} \times\left[\frac{1}{d^2}+\left(\frac{1}{d}-q\right)^2\right]^{-1}.$$

Equation (15) represents the total absorption by frozen-lattice magnons, whereas Eq. (14) is only proportional to the absorption by free-lattice magnons. To obtain the total contribution one must multiply Eq. (14) by the number of free-lattice states. Using the formula for the skin depth of periodic crystal distortion derived by Evenson and Liu, [13] one can estimate the number of such states. Taking the radiation skin depth of the metal to be 10^4 Å, clamping is found to be ineffective within this skin depth for magnons of wave number less than 10^{-4} Å^{-1}. This corresponds to about 10^3 magnon states along the hexagonal axis of the Brillouin zone of Tb or Dy metal (using sample dimensions typical of published FMR work). The total absorption by free-lattice magnons is then $W_T' = 10^3 W(0)$. The integral I_d was computed numerically, and $E(q) = E(0^+) + Cq^2$ was assumed in the integration. The microwave absorption versus external field is plotted for a variety of temperatures in Figs. 4–8 for Dy and Tb. These absorption curves were normalized by taking the maximum absorption at each temperature equal to unity. The curves are drawn only for field values above the domain-alignment field (i.e., that field necessary to align all the magnetic moments ferromagnetically). Such a domain-alignment field is finite even below the Curie temperature, since ferromagnetically aligned domains tend to align in a random fashion along the three easy axes in the basal plane.

The absorption of 10-GHz microwaves is shown in Fig. 4 for Dy metal. The absorption profile below the Curie point (85 K) is characterized by a sharp rise, followed by a long asymmetric tail which persists to very high-field values. Virtually all the absorption in the peak region is due to free-lattice-magnon processes. The ratio W_T/W_T' is less than 0.2 near the peak at the three temperatures shown. Absorption profiles above the Curie temperature have the same characteristics as the 90-K curve shown in the figure. In this curve the

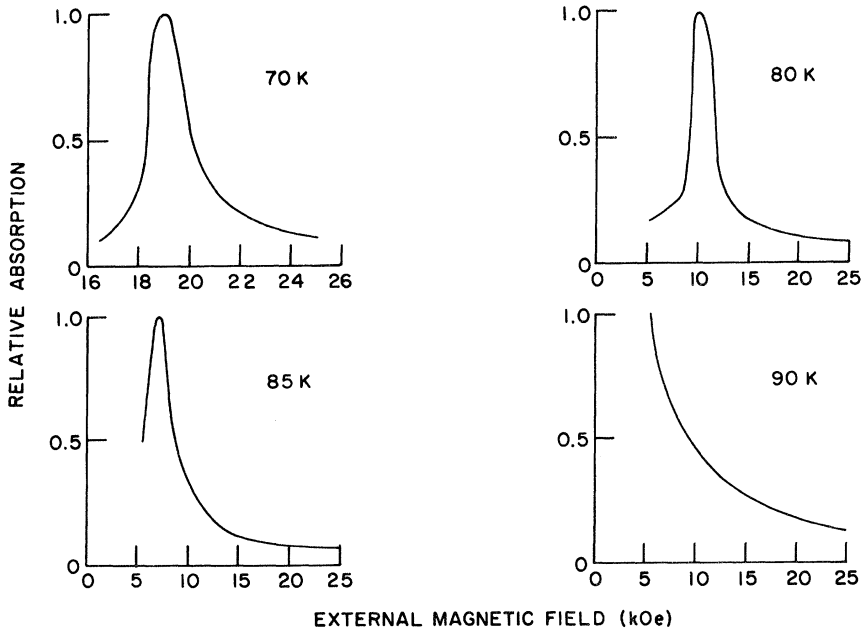

FIG. 4. Microwave absorption vs external field in Dy metal at 10 GHz.

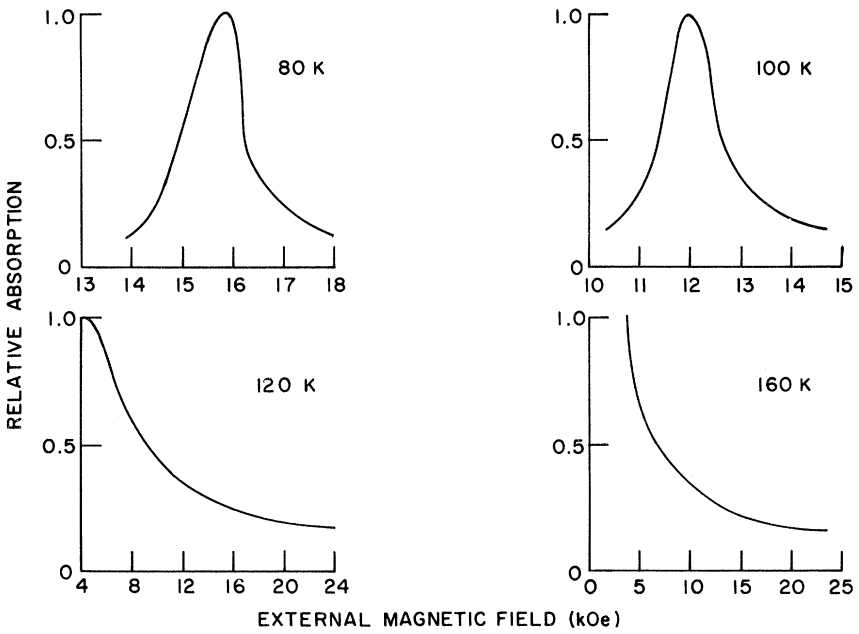

FIG. 5. Microwave absorption vs external field in Tb metal at 20 GHz.

strongest microwave absorption occurs at the "critical field," that field at which the antiferromagnetically aligned domains flip into a fan or ferromagnetic configuration. Thus in the high-temperature region, the spin-wave absorption is masked by strong domain-alignment effects. The long tail in the observed absorption[9] is due to off-resonance absorption by both free- and frozen-lattice states, the frozen-lattice states contributing most strongly. At 150 K, for example, the ratio W_T/W_T' is 4.5 over the whole field sweep. One should note a tendency for the linewidth of the absorption to narrow with increasing temperature below the Curie point. This tendency was observed by Bagguley and Liesegang,[6] and later by Rossol.[7]

The absorption of 20-GHz microwaves is shown in Fig. 5 for Tb metal. The general characteristics of the absorption are the same as for Dy. At low temperatures there is a rather sharp high-field peak. The position of this peak shifts to lower fields as temperature increases, until it falls below the domain-alignment field at 140 K. The maximum in the absorption is again masked at high temperatures by domain-alignment effects, but the long tail should still be observable, and is due primarily to off-resonance absorption by the frozen-lattice states. The absorption below 120 K is due mainly to free-lattice-magnon processes, W_T/W_T' being less than 0.2 in the peak region. This ratio increases to about 1.0 at 140 K, and frozen-lattice-magnon processes dominate the absorption above 160 K. The characteristics of the absorption profiles shown in Figs. 4 and 5 (i.e., general shape and peak positions) are observed experimentally.[6,9,11]

The absorption of 40-GHz radiation below the Curie temperature is shown versus field in Fig. 6. A barely resolvable double peak occurs below 85 K. Experimentally the double peak is not observed,[7] a fact which is not surprising because the

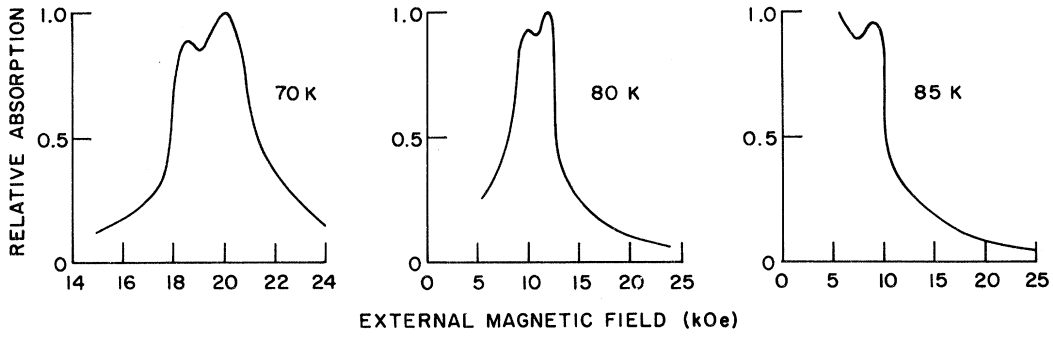

FIG. 6. Microwave absorption vs external field in Dy metal at 40 GHz.

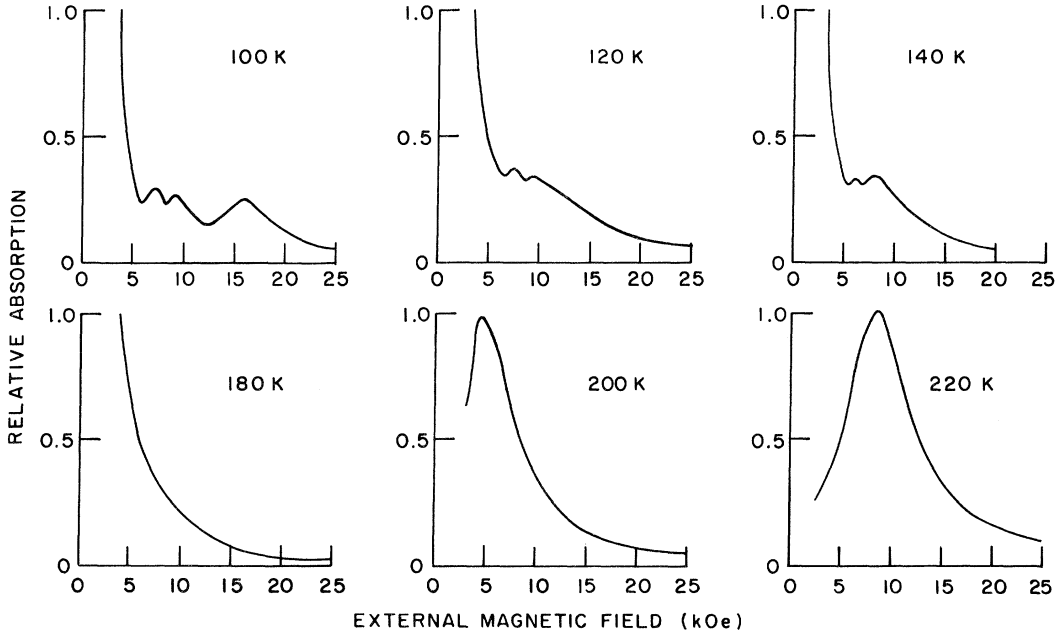

FIG. 7. Microwave absorption vs external field in Tb metal at 100 GHz.

peaks are so close, overlapping almost entirely. A strong single peak is observed, however, and occurs near the center of the calculated double peak.[7] The ratio W_T/W_T' is about 0.2 in the peak region, so that on-resonance absorption by free-lattice states is the important absorption mechanism in the production of the peak.

The absorption of 100-GHz radiation in ferromagnetic Tb is shown in Fig. 7. Below 200 K, the primary absorption occurs at the domain-alignment field due to the sharp low-field dip in the frozen-lattice-magnon gap (see Fig. 2), which makes the off-resonance absorption by frozen-lattice states quite strong. At higher fields in the low-temperature region weak structure appears due to on-resonance absorption by free-lattice magnons. This

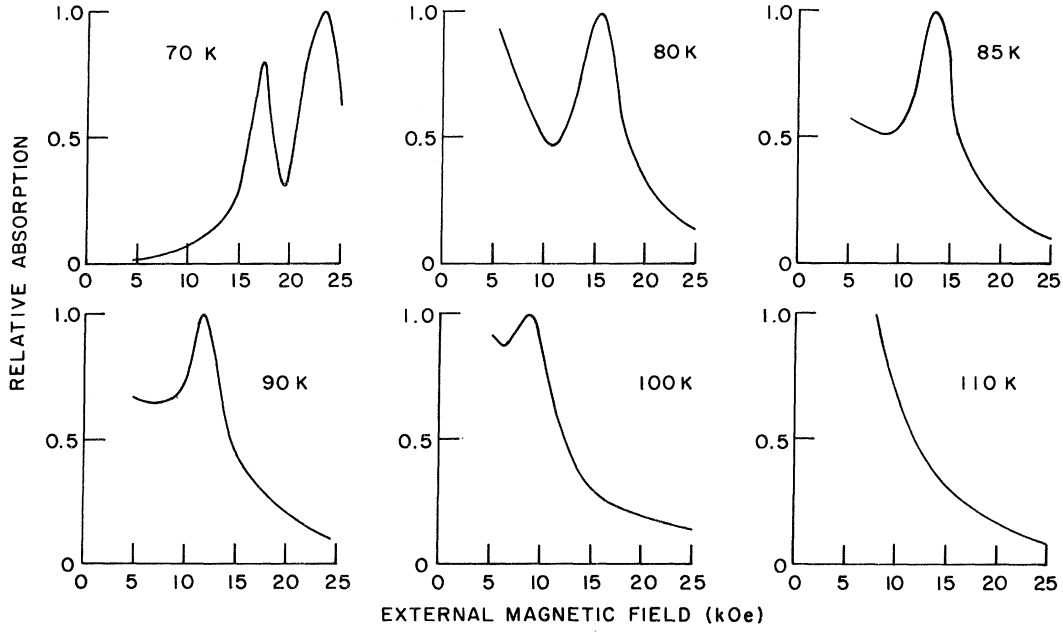

FIG. 8. Microwave absorption vs external field in Dy metal at 100 GHz.

structure, however, is not resolvable experimentally,[7] probably because of the especially low sensitivity of high-frequency microwave experiments. This weak absorption structure is also masked by the very strong absorption near domain alignment. Above 200 K, on-resonance absorption by the frozen-lattice states becomes possible. The field at which this resonance occurs increases with increasing temperature, shifting the peak to higher fields.

The absorption of 100-GHz radiation for Dy metal is shown in Fig. 8. A strong double peak appears below 80 K, and is due almost entirely to on-resonance absorption by free-lattice states. Above 85 K, the low-field peak is lost below the domain-alignment field, and at 110 K the high-field peak is lost. The curve shown at 110 K is representative of curves at higher temperatures. In this curve maximum absorption occurs at the critical field, and is followed by a long absorption tail. Off-resonance frozen-lattice processes are responsible for most of this absorption. The profiles shown in Fig. 8 have been observed in Dy for temperatures above the Curie temperature.[10] According to our calculation, the double peak should be clearly observable at 70 K, although no accurate study of ferromagnetic Dy has been made to date. Future observation of this double peak would substantiate further the evidence that free-lattice magnons play an important role in low-temperature microwave absorption.

The resonance field is defined as that field at which maximum absorption occurs. The resonance field versus temperature for Dy metal is shown in Fig. 9 for microwave frequencies of 40 and 100 GHz, along with experimental points.[7,10] The theoretical curves are obtained by taking the field values at which the calculated microwave absorption is a maximum. The average position is taken in the case of barely resolvable double peaks. At 40 GHz the resonance field increases dramatically as temperature is reduced in the ferromagnetic regime. This is due to the on-resonance absorption by free-lattice magnons, which occurs most strongly near the planar anisotropy field where $E(0)$ dips to zero (see Fig. 1). The planar anisotropy field increases with decreasing temperature, producing the sharp rise in the resonance field. The data of Rossol verify this predicted rise quite conclusively. Above the Curie temperature the 100-GHz absorption peaks occur at the critical field, so that the data of Wagner follow the critical-field curve quite well, except for a small deviation toward higher fields above 140 K.

Below the Curie temperature of Dy free-lattice-magnon absorption is the dominant process at both 40 and 100 GHz. Above the Curie temperature, frozen-lattice absorption is the dominant process at both 40 and 100 GHz. Thus, one expects the temperature dependence of the resonance field to be similar at both 40 and 100 GHz over the complete ordered regime of Dy. In ferromagnetic Tb, below 140 K, frozen-lattice-magnon processes dominate 100-GHz absorption, producing a peak at the domain-alignment field; whereas free-lattice-magnon processes dominate 20-GHz absorption, producing a peak at the effective planar anisotropy field. Therefore, the theory predicts a striking difference in the behavior of the resonance-field curves at the two frequencies. The resonance field versus temperature for Tb metal at 20 and 100 GHz is shown in Fig. 10, along with the experimental points at 24 GHz.[8,11] There is a dramatic increase of 8 kOe in the 20-GHz curve between 140 and 100 K. Over the same temperature interval, the 100-GHz curve changes less than 1 kOe. The experimental points fall almost exactly on the theoretical curves, providing an extremely strong confirmation of the

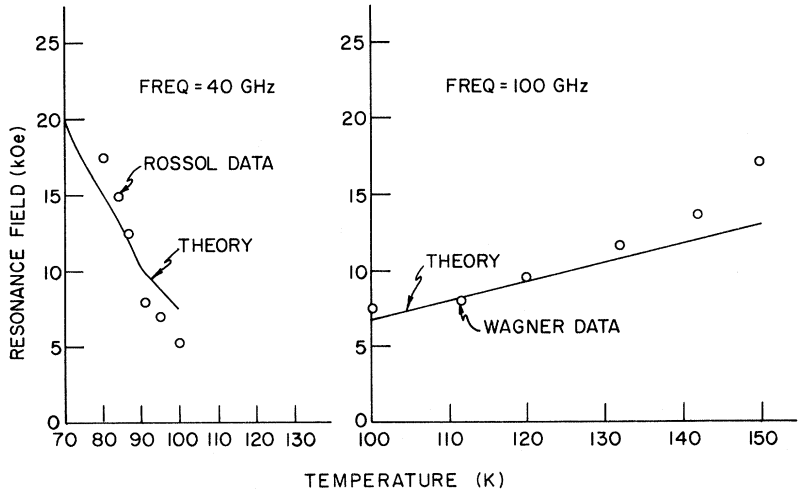

FIG. 9. Resonance field vs temperature for Dy metal.

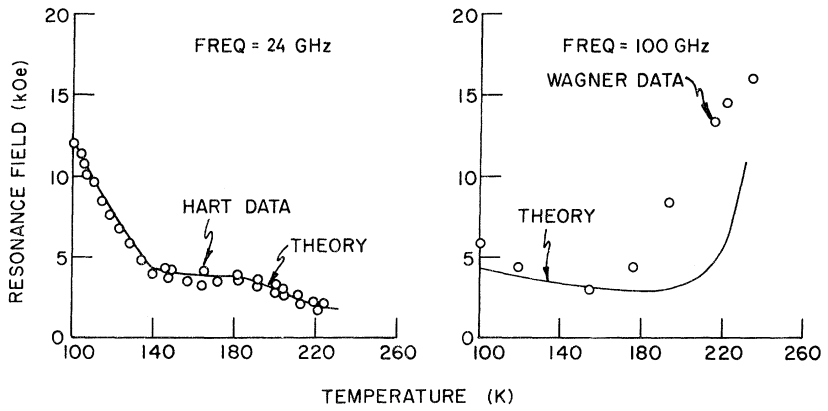

FIG. 10. Resonance field vs temperature for Tb metal.

theory.

One notes that good experimental agreement is attained in both metals using the statically measured planar anisotropy constants[21] with a temperature renormalization of $\hat{I}_{13/2}$ for Dy and $\hat{I}_{9/2}\hat{I}_{5/2}$ for Tb. This result differs somewhat from the earlier results of Cooper, [2] presumably because of the inclusion of the field dependence of the magnetization in the calculation of the spin-wave gaps. A neutron-diffraction study of Tb [5] has verified that the planar anisotropy of that metal is of magnetoelastic origin, so that the temperature renormalization $\hat{I}_{9/2}\hat{I}_{5/2}$ is well justified. The renormalization $\hat{I}_{13/2}$ for Dy assumes that the planar anisotropy arises from crystal field symmetry in this metal. Such an assumption seems to be well justified by the excellent agreement of the theory with microwave-absorption data. A neutron-diffraction study of Dy, similar to that done for Tb, seems appropriate at this time to see if there is indeed a difference in the origin of the planar anisotropy in these metals. The microwave experiments point very strongly to this conclusion.

II. MAGNON-PHONON INTERACTION

A. Introduction

In Sec. I we computed the effects of uniform magnetostriction on the spin-wave energies. In this section, we calculate the effect of arbitrary vibrations of the crystal ions about the uniformly strained configuration produced by the spin order. In general, the vibrations produce nonuniform strains which couple locally to the spin system through the local magnetoelastic interaction of Evenson and Liu. [13] Normal modes of lattice and spin vibrations couple strongly when vibrational frequencies are nearly equal, producing mixed spin-lattice modes. The magnetoelastic coupling removes the degeneracy of the unperturbed spin and lattice modes at the point where the dispersion curves cross, and the size of the branch splitting is a measure of the coupling strength.

Neutron-diffraction studies of excitation spectra in Tb and Tb alloys show a large splitting between acoustical-magnon (MA) and transverse-optical-phonon (TO) branches in the region of the Brillouin zone where the energies of the unperturbed modes are equal. [18, 22] Very recent measurements also show a smaller splitting between MA and transverse acoustical (TA) branches. [23] These experimental results are shown in Fig. 11. In Sec. II B we calculate the latter splitting using the local spin-strain interaction, and good agreement with experiment is attained. This interaction fails to couple acoustical to optical modes, however, and therefore does not account for the observed MA-TO splitting. In Sec. II C a possible mechanism for the coupling of these modes is proposed.

B. Calculation of Splitting

First we compute the ϵ-representation terms of the magnetoelastic interaction. The local strain functions for this representation are

$$\mathcal{E}^{\epsilon}_{1f} = \tfrac{1}{2}\sum_{\delta}\left[\delta_x(r^z_f - r^z_{f+\delta}) + \delta_z(r^x_f - r^x_{f+\delta})\right],$$
$$\mathcal{E}^{\epsilon}_{2f} = \tfrac{1}{2}\sum_{\delta}\left[\delta_y(r^z_f - r^z_{f+\delta}) + \delta_z(r^y_f - r^y_{f+\delta})\right]. \tag{16}$$

Here $f = (l, s)$ labels the position of the fth atom in the crystal, and δ labels the positions of its 12 nearest neighbors.

From lattice-vibration theory the second quantized form of the components of displacement from the unstrained equilibrium positions is given by

$$r^i_{ls} = \sum_{\rho,\vec{q}} R_{\rho,\vec{q}}\, V^{\vec{q}\rho}_{is}\, e^{i\vec{q}\cdot\vec{l}}\,(\beta_{-\vec{q}\rho}{}^{\dagger} + \beta_{\vec{q}\rho}). \tag{17}$$

Here $i = (x, y, z)$ and $s = (0, \frac{1}{2}c)$ label the two atoms of the unit cell, ρ labels the mode of vibration, and l labels the unit cell. The quantity $R_{\rho\vec{q}} = (\hbar/Nm\omega_{\rho\vec{q}})^{1/2}$, where N is the number of unit cells, m is the mass of an ion, and $\omega_{\rho\vec{q}}$ is the frequency of a normal mode of crystal vibration. The quantities $v^{\vec{q}\rho}_{is}$ are the components of the polarization vector of the lattice wave, and β and β^{+} are the annihilation and creation

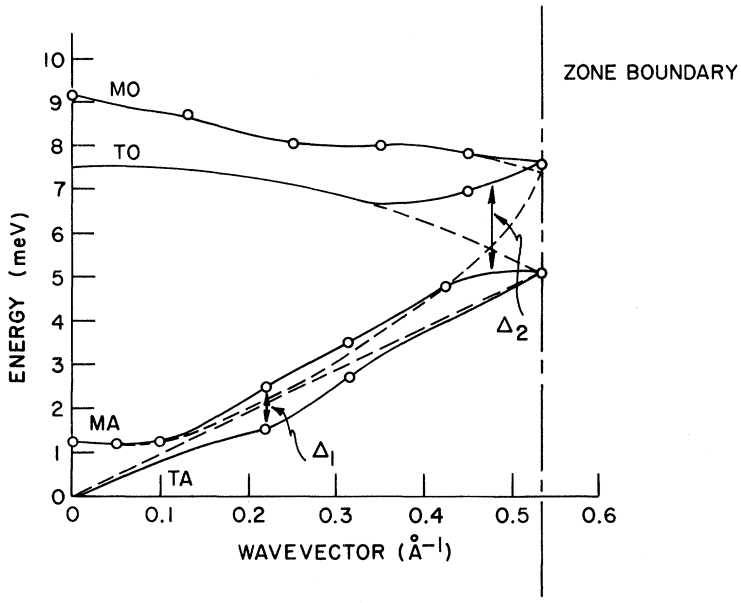

FIG. 11. The magnon (MA, MO) and transverse-phonon (TA, TO) dispersion curves for Tb in the c direction at 79 K. The magnon-phonon interaction causes a mixing of modes and splittings at the crossing points of the unperturbed dispersion curves (indicated by dashed lines).

operators for the phonons. The components of the polarization vector must satisfy the following orthonormality condition:

$$\sum_{i,s} (v_{is}^{\vec{q}\rho})^* (v_{is}^{\vec{q}\rho'}) = \delta_{\rho\rho'} . \tag{18}$$

In order to compare the results of the calculation with measurements on Tb, we assume the lattice modes to be propagating along the $\hat{c}$ axis of a hcp crystal, and to be transverse polarized along the $\hat{a}$ axis in the basal plane. The Cartesian coordinates appearing in Eqs. (16) are defined with $\hat{x}$ along $\hat{a}$ and $\hat{z}$ along $\hat{c}$. For such lattice waves, the solution to Eq. (18) for the polarization vectors is

$$\begin{aligned} v_{x0}^{q\rho} &= \frac{1}{\sqrt{2}}\hat{a} \qquad (\rho = 1, 2) , \\ v_{xc/2}^{q1} &= \frac{1}{\sqrt{2}} e^{iqc/2}\hat{a} , \\ v_{xc/2}^{q2} &= \frac{-1}{\sqrt{2}} e^{iqc/2}\hat{a} , \\ v_{ys}^{q\rho} &= v_{zs}^{q\rho} = 0 \qquad (s = 0, \tfrac{1}{2}c; \qquad \rho = 1, 2) . \end{aligned} \tag{19}$$

Then, using Eqs. (19) in Eq. (17), we find the local strains of Eqs. (16) to be

$$\begin{aligned} \mathcal{E}_{1f}^{\epsilon} &= \frac{3ic}{2\sqrt{2}} \sum_{q,\rho} R_{\rho\vec{q}} e^{i\vec{q}\cdot\vec{r}} \left(\sin\frac{qc}{2}\right) (\beta_{-q\rho}^{\dagger} + \beta_{q\rho}) \eta_{f\rho} , \\ \mathcal{E}_{2f}^{\epsilon} &= 0 , \end{aligned} \tag{20}$$

where

$$\eta_{f1} = \eta_{f2} = 1 \qquad \text{if } f = (l, 0)$$

and

$$\eta_{f1} = -\eta_{f2} = 1 \qquad \text{if } f = (l, \tfrac{1}{2}c) .$$

The summation on q is taken along the c axis of the Brillouin zone in the single-zone scheme. The hcp structure is considered to be made of two identical interpenetrating hexagonal sublattices. Two kinds of spin deviation operators a_f and b_f are introduced corresponding to each of the two sublattices.[24] Then the spin functions of the ϵ representation are transformed to spin-deviation operators as follows:

$$\begin{aligned} S_{1f}^{\epsilon} &= -(\tfrac{1}{2}S^3)^{1/2}(a_f^{\dagger} + a_f), \qquad f = (l, 0) \\ &= -(\tfrac{1}{2}S^3)^{1/2}(b_f^{\dagger} + b_f), \qquad f = (l, \tfrac{1}{2}c) . \end{aligned} \tag{21}$$

Using Eqs. (20) and (21) in the local magnetoelastic Hamiltonian and summing over lattice sites we obtain

$$H_{\text{me}}^{\epsilon} = -\frac{\tilde{B}^{\epsilon}(NS^3)^{1/2} i}{2\sqrt{2}c} \sum_{\rho q} R_{\rho q}\left(\sin\frac{qc}{2}\right)(\beta_{-q\rho}^{\dagger} + \beta_{q\rho}) \times [a_q^{\dagger} + a_{-q} + \lambda_{\rho}(b_q^{\dagger} + b_{-q})] , \tag{22}$$

where

$$\lambda_{\rho} = 1 \qquad \text{if } \rho = 1$$

and

$$\lambda_{\rho} = -1 \qquad \text{if } \rho = 2 .$$

Here a_q and b_q are the Fourier transforms of the spin-deviation operators a_f and b_f.

The terms in the magnetoelastic Hamiltonian that transform according to the γ and α representations are calculated in an exactly similar way. A surprising result is that $H_{\text{me}}^{\gamma} = 0$. The local strains are zero in this case, due to the choice $\vec{q} = q\hat{c}$ and the hcp symmetry of the crystal. The spin functions of the α representation all involve bilinear combinations of the magnon operators, so H_{me}^{α} contains only processes that do not conserve

particle number, and which contribute only to broadening effects.

Let H_{m-p} denote the total second-quantized Hamiltonian relevant to mode mixing:

$$H_{m-p}=\tfrac{1}{2}\sum_{qj\rho}\{A_{qj}(a_q^\dagger a_q+b_q^\dagger b_q)+\tfrac{1}{2}B_{qj}(a_q^\dagger a_{-q}^\dagger+a_q a_{-q}+b_q^\dagger b_{-q}^\dagger+b_q b_{-q})+\hbar\omega_{q\rho}\beta_{q\rho}^\dagger\beta_{q\rho}+\Delta_{q\rho}(\beta_{-q\rho}^\dagger+\beta_{q\rho})\times[(a_q^\dagger+a_{-q})+\lambda_\rho(b_q^\dagger+b_{-q})]\}, \quad (23)$$

where

$$\Delta_{q\rho}=-\frac{\tilde{B}^e(NS^3)^{1/2}i}{2\sqrt{2}\,c}\left(\sin\frac{qc}{2}\right)R_{\rho q}\,.$$

The quantity $\hbar\omega_{\rho q}$ is the unperturbed phonon energy, and A_{qj} and B_{qj} are the coefficients that appear in Eq. (7) with a subscript $j=1, 2$ added to denote acoustical- or optical-magnon branches, respectively. (The earlier discussion was in the double-zone scheme using a Bravais lattice.) The factor $\frac{1}{2}$ in Eq. (23) is inserted to prevent double counting. The boson operators a_q and b_q are a mixture of acoustical- and optical-magnon-annihilation operators. We define operators c_q and d_q by the following transformation:

$$a_q=(1/\sqrt{2})(c_q+d_q)\,,\qquad b_q=(1/\sqrt{2})(c_q-d_q)\,. \quad (24)$$

Expressing H_{m-p} in terms of these new boson operators we obtain

$$H_{m-p}=\tfrac{1}{2}\sum_{qj\rho}\{A_{qj}(c_q^\dagger c_q+d_q^\dagger d_q)+\tfrac{1}{2}B_{qj}(c_q^\dagger c_{-q}^\dagger+c_q c_{-q}+d_q^\dagger d_{-q}^\dagger+d_q d_{-q})+\hbar\omega_{\rho q}\beta_{q\rho}^\dagger\beta_{q\rho}+\sqrt{2}\,\Delta_{q\rho}(\beta_{-q\rho}^\dagger+\beta_{q\rho})\times[(c_q^\dagger+c_{-q})\delta_{\rho1}+(d_q^\dagger+d_{-q})\delta_{\rho2}]\}\,. \quad (25)$$

Here $\delta_{\rho1}$ and $\delta_{\rho2}$ are Kronecker δ's. Finally, we make a Bogoliubov transformation of the operators c_q and d_q to magnon-creation and -annihilation operators:

$$c_q=u_{1q}\alpha_{1q}-v_{1q}\alpha_{1,-q}^\dagger\,,\qquad d_q=u_{2q}\alpha_{2q}-v_{2q}\alpha_{2,-q}^\dagger\,. \quad (26)$$

Here α_{1q} and α_{2q} are the annihilation operators for acoustical and optical magnons, respectively. The coefficients of the transformation satisfy relations analogous to Eqs. (12). Substitution of Eqs. (26) into Eq. (25) yields

$$H_{m-p}=\sum_{j,q}E_j(q)\alpha_{jq}^\dagger\alpha_{jq}+\sum_{\rho,q}\hbar\omega_{\rho q}\beta_{q\rho}^\dagger\beta_{q\rho}+\sum_{j\rho q}\left(\frac{E_j(q)}{2(A_{qj}+B_{qj})}\right)^{-1/2}\Delta_{q\rho}\delta_{j\rho}(\alpha_{jq}^\dagger+\alpha_{j,-q})(\beta_{\rho,-q}^\dagger+\beta_{\rho q})\,. \quad (27)$$

By virtue of the Kronecker δ, $\delta_{j\rho}$, that appears in Eq. (27), the magnetoelastic interaction of Evenson and Liu [Eq. (1)] fails to account for the coupling of acoustical and optical modes. This interaction was originally devised in order to describe static effects, and so couples only local displacements to the spin system. In the excited states of the lattice, however, dynamic quantities, such as lattice angular momentum, may couple to the spins. In Sec. IIC, it is shown that a kind of "L-S coupling" does, in fact, couple the acoustical magnons to the optical phonons, giving rise to a splitting. This mechanism, however, does not lead to any coupling of acoustical modes, so let us use the mode-mixing Hamiltonian H_{m-p} to calculate the splitting between the TA and MA branches.

For the mixing of these specific modes H_{m-p} reduces to

$$H_{m-p}=\textstyle\sum_q E(q)\alpha_q^\dagger\alpha_q+\sum_q\hbar\omega_q\beta_q^\dagger\beta_q+\sum_q\Delta_q'(\alpha_q^\dagger+\alpha_{-q})(\beta_{-q}^\dagger+\beta_q)\,. \quad (28)$$

Here $\Delta_q'=[E(q)/2(A_q+B_q)]^{-1/2}\Delta_q$, and the mode labels ρ and j are suppressed. We diagonalize this Hamiltonian by defining a new annihilation operator:

$$\gamma_q=t_1\alpha_{-q}+t_2\alpha_q^\dagger+t_3\beta_{-q}+t_4\beta_q^\dagger\,.$$

The imposition of the condition $[\gamma_q, H_{m-p}]=\Omega_q\gamma_q$ gives four homogeneous equations in the coefficients t_1, t_2, t_3, t_4. The quantity Ω_q is the energy of the mixed phonon-magnon mode. The solution of the Heisenberg equation of motion is nontrivial if the following condition on the secular determinant is met:

$$\begin{vmatrix}[E(q)-\Omega_q] & 0 & \Delta_q' & \Delta_q'\\ 0 & [E(q)+\Omega_q] & \Delta_q' & \Delta_q'\\ \Delta_q'^* & \Delta_q'^* & (\hbar\omega_q-\Omega_q) & 0\\ \Delta_q'^* & \Delta_q'^* & 0 & (\hbar\omega_q+\Omega_q)\end{vmatrix}=0\,. \quad (29)$$

In writing Eq. (29) we use $\Delta_{-q}'=\Delta_q'^*$. The determinant may be simplified easily, and reduces to the following equation for the eigenvalues of the mixed-mode state:

$$\Omega_q^4-\Omega_q^2\{[E(q)]^2+(\hbar\omega_q)^2\}+(\hbar\omega_q)^2\times[E(q)]^2-4\hbar\omega_q|\Delta_q'|^2E(q)=0\,. \quad (30)$$

One observes strong mixing when $E(Q)=\hbar\omega_Q$, Q being the wave number at which the branches "kiss." In this case Eq. (30) has the solution

$$\Omega_Q=E(Q)\pm|\Delta_Q'|\,;$$

then the energy splitting Δ_2 at Q is

$$\Delta_2=2|\Delta_Q'|=\frac{\tilde{B}^e}{c}\left(\frac{\hbar^2S^3(A_Q+B_Q)}{m[E(Q)]^2}\right)^{1/2}\sin\frac{Qc}{2}\,. \quad (31)$$

Taking $E(Q)$ to be 2.0 meV and $Q=0.25$ Å^{-1} we find

$$\Delta_2=0.86\text{ meV}\,.$$

This compares well with the observed splitting

and agrees with the results of an independent calculation by Jensen.[23]

C. Mechanism for Coupling of MA and TO Modes in Tb

In this section a mechanism is proposed which couples acoustical magnons to optical phonons along the $\hat{c}$ axis of a hcp crystal near the edge of the Brillouin zone. Such coupling results in a splitting of the dispersion relations of these modes as observed in Tb metal, and cannot be explained using a formulation of magnetoelasticity which couples the spin system to local strain fields.

In order to see how the lattice couples to the spin system, one must look in detail at the way the ions vibrate when a TO mode is excited along the $\hat{c}$ axis near the Brillouin-zone edge. One sublattice of atoms, say $f=(l, 0)$, remains nearly stationary, whereas the other sublattice, $f=(l, \frac{1}{2}c)$, vibrates with nearest-neighbor planes on the sublattice, being nearly 180° out of phase. Thus, angular momentum is generated by the vibrating sublattice, which can be coupled to the spin moments on the stationary sublattice. This formulation yields a kind of spin-lattice L-S coupling, and it can be written phenomenologically as follows:

$$H_{\text{me}}=\sum_{f\delta} A[(\vec{\mathrm{R}}_f-\vec{\mathrm{R}}_{f+\delta})\times(\vec{\mathrm{v}}_f-\vec{\mathrm{v}}_{f+\delta})]\cdot\vec{\mathrm{S}}_f\ . \tag{32}$$

Here $\vec{\mathrm{R}}_f$ is the position vector of the fth site, $\vec{\mathrm{v}}_f$ is the velocity of the fth site, and A is an unspecified coupling constant. We apply Eq. (32) to Tb metal, assuming that the net magnetization is confined to the basal plane along the easy $\hat{a}$ axis. We take the polarization of the TO phonons to be in an arbitrary planar direction, specified by angle θ to the $\hat{a}$ axis. Then, assuming $\vec{\mathrm{v}}_f\approx 0$, the part of Eq. (32) which leads to magnon-phonon mixing is given by

$$H_{m\text{-}p}=\sum_{f\delta}(\mp)\frac{Ac}{2}\,v_{f+\delta}S_f^y\cos\theta\ . \tag{33}$$

Here the upper (lower) sign is used when summing on atoms in the upper (lower) nearest-neighbor planes of the fth atom. The quantity c is a lattice constant. The quantity S_f^y is the component of the spin perpendicular to the $\hat{a}$ axis, and may be expressed as a linear combination of Fourier-transformed spin-deviation operators of the sublattice $f=(l, 0)$:

$$S_f^y=i\,(\tfrac{1}{2}NS)^{1/2}\textstyle\sum_k(a_k^\dagger e^{-i\vec{k}\cdot\vec{l}}-a_k e^{i\vec{k}\cdot\vec{l}})\ .$$

Then noting that the Fourier components of the displacement $\vec{\mathrm{r}}_{f+\delta}$ depend on time, according to the factor $e^{i\omega_q t}$, we use Eq. (17) to transform $\vec{\mathrm{v}}_{f+\delta}=(d/dt)(\vec{\mathrm{r}}_{f+\delta})$ to phonon operators. Then, after summation over f and δ, Eq. (33) becomes

$$H_{m\text{-}p}=\tfrac{3}{2}cAi\,(NS)^{1/2}(\cos\theta)\textstyle\sum_q\omega_q R_q(\sin\frac{1}{2}qc)(\beta_{-q}^\dagger+\beta_q)(a_{-q}-a_q^\dagger)\ . \tag{34}$$

Here the optical-phonon index, $\rho=2$, is suppressed. The spin operators of Eq. (34) may be transformed to a linear combination of acoustical- and optical-magnon operators by using Eqs. (24) and (26). Then the part of Eq. (34) which couples TO phonons to acoustical magnons becomes

$$H_{\text{TO-MA}}=\textstyle\sum_q\Delta_q(\beta_{-q}^\dagger+\beta_q)(\alpha_{-q}-\alpha_q^\dagger)\ . \tag{35}$$

Here the acoustical-magnon index, $j=1$, is suppressed. The strength of the interaction, Δ_q, in the region of strong coupling is written explicitly as

$$\Delta_Q=\frac{3Aci}{4}\left(\frac{S(A_Q+B_Q)}{m}\right)^{1/2}\left(\sin\frac{Qc}{2}\right)|\cos\theta|\ , \tag{36}$$

where Q is the wave number at which the acoustical and optical branches cross. The unperturbed TO phonons are degenerate with respect to polarization direction, so we consider θ as uniformly distributed between zero and $\pi/2$ with probability density $P(\theta)=(\frac{1}{2}\pi)^{-1}$. Then the splittings Δ_Q are distributed with density $P(|\cos\theta|)=2/(\pi\sin\theta)$. This is reflected in the energy-absorption profiles of a neutron-diffraction experiment which should show sharp peaks in the neutron scattering by quasiparticles in the region of maximum splitting (i.e., for $\theta=0$). The peak should be asymmetric, dropping sharply to zero for energies greater than that given by maximum splitting, and more gradually to a small minimum at the unperturbed energy of the phonon and magnon excitations.

One may account for the natural linewidth of the quasiparticle states by allowing the δ-function distribution of each value $|\cos\theta|$ to broaden into a Lorentzian distribution. Letting $x=|\cos\theta|$, the probability density for the unbroadened spectrum is $P(x)=\int dr\,\delta(x-r)P(r)$. In this expression we make the replacement

$$\delta(x-r)\to(\gamma/\pi)\,[(x-x')^2+\tfrac{1}{4}\gamma^2]^{-1}\ ,$$

where γ is the linewidth of the spectrum. The distribution which allows for broadening may then be written as

$$P(x)=(2\gamma/\pi)\int_0^1 dr\,(1-r^2)^{-1/2}(r^2-2xr+x^2+\tfrac{1}{4}\gamma^2)^{-1}\ . \tag{37}$$

The integral in Eq. (37) has been computed numerically and shows a strong asymmetric peak in the region of maximum splitting ($\theta=0$).[25] If the model proposed here has any validity, this line shape should be a characteristic of the neutron-energy-absorption profiles.

In order to agree with the observed splitting in Tb, the value of A in Eq. (36) must be of order 10^{-18} g/sec. We calculated A assuming that an effective field at the stationary sites is generated by current created by the vibrating neighbor ions. This classical approach yields a value A that is four or-

ders of magnitude too small. A much stronger interaction might be produced if the conduction electrons mediate the interaction between the lattice and the local spins, in analogy to the strong indirect exchange interaction which couples the local spins together in Tb. Mediation by itinerant 5*d* electrons is plausible, since their large orbital moments can couple effectively with the field produced by the vibrating lattice.

ACKNOWLEDGMENTS

We wish to thank Dr. Timothy Wagner and Dr. Lynn Hart for many useful discussions concerning the FMR studies in Tb and Dy.

---

*Work performed in the Ames Laboratory of the U. S. Atomic Energy Commission, Contribution No. 2890.

[1]E. A. Turov and V. G. Shavrov, Fiz. Tverd. Tela 7, 217 (1965) [Sov. Phys. Solid State 7, 166 (1965)].

[2]B. R. Cooper, Phys. Rev. 169, 281 (1968).

[3]E. Callen and H. Callen, Phys. Rev. 139, A455 (1965).

[4]H. Marsh and A. J. Sievers, J. Appl. Phys. 40, 1563 (1969).

[5]M. Nielsen, H. B. Møller, P. A. Lindgård, and A. R. Mackintosh, Phys. Rev. Letters 25, 1451 (1970).

[6]D. M. S. Bagguley and J. Liesegang, Proc. Roy. Soc. (London) A300, 497 (1967).

[7]F. C. Rossol, Ph. D. thesis (Harvard University, 1966) (unpublished); F. C. Rossol and R. V. Jones, J. Appl. Phys. 37, 1227 (1966).

[8]T. K. Wagner and J. L. Stanford, Phys. Rev. 184, 505 (1969).

[9]T. K. Wagner and J. L. Stanford, Phys. Rev. B 1, 4488 (1970).

[10]T. K. Wagner and J. L. Stanford, Phys. Rev. (to be published).

[11]L. Hart and J. L. Stanford, Phys. Rev. Letters 27, 674 (1971).

[12]D. T. Vigren and S. H. Liu, Phys. Rev. Letters 27, 676 (1971).

[13]W. E. Evenson and S. H. Liu, Phys. Rev. 178, 783 (1969).

[14]A. E. Clark, B. F. DeSavage, and R. Bozorth, Phys. Rev. 138, A216 (1965).

[15]B. F. DeSavage and A. E. Clark, Proceedings of the Fifth Rare Earth Conference, Ames, Iowa, 1965 (unpublished).

[16]J. J. Rhyne and S. Legvold, Phys. Rev. 138, A507 (1965).

[17]E. S. Fisher and D. Dever, Trans Met. Soc. AIME 239, 48 (1967).

[18]H. B. Møller, M. Nielsen, and A. R. Mackintosh, J. Appl. Phys. 41, 1174 (1970).

[19]D. R. Behrendt and S. Legvold, Phys. Rev. 109, 1544 (1958).

[20]D. E. Hegland, S. Legvold, and F. H. Spedding, Phys. Rev. 131, 158 (1963).

[21]J. J. Rhyne and A. E. Clark, J. Appl. Phys. 38, 1379 (1967).

[22]H. B. Møller, J. C. Houmann, and A. R. Mackintosh, Phys. Rev. Letters 19, 312 (1967).

[23]J. Jensen, Intern. J. Magnetism 1, 271 (1971).

[24]M. S. S. Brooks, D. A. Goodings, and H. I. Ralph, J. Phys. C 1, 132 (1968).

[25]R. A. Reese and R. G. Barnes, Phys. Rev. 163, 465 (1967).